

Ginzburg-Landau Model and Single-Mode Operation of a Free-Electron Laser Oscillator

C. S. Ng and A. Bhattacharjee

Department of Physics and Astronomy, The University of Iowa, Iowa City, Iowa 52242

(Received 28 September 1998)

It is shown that the radiation field in a long-pulse, low-gain free-electron laser oscillator obeys the complex Ginzburg-Landau equation. The question of single-mode operation is investigated by analysis and simulation, and the results are compared with experiments at the University of California at Santa Barbara, as well as the Dutch fusion free-electron-maser experiment. It is shown that the intervention of a frequency-dependent reflection coefficient can facilitate the realization of single-mode operation. [S0031-9007(99)08757-8]

PACS numbers: 41.60.Cr, 42.65.Tg, 52.35.Mw

In a free-electron laser (FEL) oscillator, the intensity of the radiation field is built up over many passes of the radiation in a resonator cavity at the expense of the energy of a relativistic electron beam. Several cavity modes are usually excited due to the interaction of the electron and the optical beam. This paper is motivated by two principal questions: (i) What is the equation governing the nonlinear dynamics of the radiation field when multiple modes are excited. (ii) What are the conditions under which a single-mode state emerges spontaneously from the nonlinear evolution of a broad spectrum of unstable modes competing for the energy of the electron beam?

The theory developed in this paper is applicable to low-gain FEL oscillators driven by long-pulse electron beams. These devices exhibit a strong tendency to evolve into a single-mode state [1–3]. The linewidths realized can be very small, making them ideal for demanding applications such as spectroscopy or isotope separation. For such devices, we demonstrate that the radiation field amplitude $A(z, t)$ can be modeled by the complex Ginzburg-Landau equation (GLE),

$$\frac{\partial A}{\partial z} = A + (1 + ic_1) \frac{\partial^2 A}{\partial t^2} - (1 + ic_2) |A|^2 A, \quad (1)$$

where z is the coordinate along the axis of the undulator, t is time, and c_1 and c_2 are real parameters calculated by the theory. We then apply the model to two different FEL devices—one at the University of California at Santa Barbara (UCSB) [1,2] and the other at the Dutch FOM-Institute for Plasma Physics [3]. Whether single-mode operation was truly realized within the lifetime of the electron pulse in the UCSB experiment has been a source of theoretical controversy in the past [4,5]. Based on a large number of high-resolution simulations of the GLE with random initial conditions, we conclude that, in the absence of frequency selective feedback, a single-mode state was most probably not realized in the UCSB experiment. We also apply the GLE, with some modifications, to the Dutch fusion free-electron maser (FEM) experiment which has recently reported single-mode operation [3]. We show that, although it

takes a very long time to realize a single mode in the absence of any frequency discrimination, the intervention of a frequency-dependent reflection coefficient may have facilitated the realization of a single-mode state within the lifetime of the electron beam in the Dutch experiment.

In earlier work, we have derived the GLE [6,7] from the FEL amplifier equations in the high-gain Compton regime. In this paper, we derive the GLE from the low-gain oscillator equations. In so doing, we make a strong case for the universal applicability of the GLE to a long-pulse FEL, independent of whether the FEL is configured as an oscillator or an amplifier.

We begin with the formulation used in [5] (which originated from [8]). We define the normalized signal amplitude by the relation

$$a = \frac{qA}{mc^2} \left(\frac{\omega L}{c} \right)^2 \frac{K(1 + K^2/2)}{[\gamma_R^2 - (1 + K^2/2)]^2},$$

where q , m , γ_R , and c are the electron charge, mass, relativistic factor, and speed of light, respectively, ω is the reference frequency of the radiation, $K = qA_w/mc^2\gamma_R$ is the wiggler parameter, L is the length of the interaction region, and A_w is the magnetic potential of the wiggler. We represent a by the Fourier series

$$a(\tau_s, \tau_0) = \sum_{n=-\infty}^{\infty} a_n(\tau_s) \exp(-in\pi\tau_0). \quad (2)$$

In (2), the time dependence of a is separated into a fast time τ_0 associated with the time of transit of the radiation through the empty cavity, and a slower time τ_s associated with the decay time of the radiation in the empty cavity. Specifically, we write $\tau_0 = tv_g/L_c$, where t is the physical time, L_c is the cavity length, v_g is the axial group velocity, and $\tau_s = tv_g/2L_c$, where v is the fraction of the power lost from the radiation field per round trip. Note that a is a periodic function of τ_0 , with a period of 2. The evolution of a in slow time is given by the equation

$$\frac{da_n}{d\tau_s} + \frac{1}{2} a_n = -\frac{i\hat{I}}{4v} \int_0^2 \frac{d\tau_0}{2} \int_0^1 d\xi \times \langle \exp\{-i[\psi - n\pi(\varepsilon\xi + \tau_0)]\} \rangle, \quad (3)$$

where

$$\hat{I} = \frac{4\pi j L^3 \omega}{I_A v_g} \frac{K(1 + K^2/2)}{[\gamma_R^2 - (1 + K^2/2)]^2},$$

is the normalized current. Here $I_A = \gamma_R \beta_z m c^3 / q$ is the so-called Alfvén limiting current, j is the effective beam current density, $\beta_z = v_z / c$ is the normalized electron axial velocity, $\xi = z / L$ is the normalized axial coordinate, $\varepsilon = L(v_g - v_z) / L_c v_z$ is the slippage parameter, and $\psi = (k_w + k_z)z - \omega t$ is the relative phase of an electron, with k_w, k_z denoting the wave number of the wiggler and the radiation field. The angle bracket in (3) represents an ensemble average over entrance phases

ψ_0 , assumed to be uniformly distributed between 0 and 2π . The phase ψ satisfies the one-dimensional pendulum equation,

$$\begin{aligned} \frac{dp}{d\xi} &\equiv \frac{d^2\psi}{d\xi^2} \\ &= \text{Im} \left(\sum_{n=-\infty}^{\infty} a_n \exp\{i[\psi - n\pi(\varepsilon\xi + \tau_0)]\} \right), \end{aligned} \quad (4)$$

subject to the boundary condition $d\psi/d\xi|_{\xi=0} = p_0 = \text{const}$. Equations (3) and (4) are the basic equations underlying the numerical simulations discussed in [5].

We define $Q \equiv \langle \exp(-i\psi) \rangle$. Using (2), we can rewrite (3) as

$$\frac{\partial a}{\partial \tau_s} + \frac{1}{2} a = -\frac{i\hat{I}}{4v} \int_0^1 d\xi Q[p_0, \xi, a(\tau_s, \tau_0 - \varepsilon\xi), \varepsilon \partial a(\tau_s, \tau_0 - \varepsilon\xi) / \partial \tau_0, \dots]. \quad (5)$$

Expressing ψ in a Taylor series $\psi(\xi) = \sum_{n=0}^{\infty} \xi^n (d^n \psi / d\xi^n)|_{\xi=0} / n!$, we obtain, in the low-gain approximation,

$$\begin{aligned} \exp[-i\psi(\xi)] &= \exp[-i(\psi_0 + p_0\xi)] \sum_{m=0}^{\infty} \frac{1}{m!} \\ &\times \left[-i \sum_{n=2}^{\infty} \frac{\xi^n}{n!} \frac{d^n \psi}{d\xi^n} \Big|_{\xi=0} \right]^m. \end{aligned}$$

By (4), the m th term in the above series is $O(a^m)$. We consider the case of small a , and so keep only terms up to $O(a^3)$. The cubic nonlinearity in the GLE is stabilizing, predicts a saturated power level [6] for the FEL, and thus enables us to apply the GLE even when a is of the order of unity. The effect of sideband instabilities, which appear when a is much larger, will not be considered here and is left to future work.

It can be easily shown that terms containing odd powers of a are the only ones to survive the ensemble average. So we obtain

$$\begin{aligned} Q &\approx \left\langle e^{-i(\psi_0 + p_0\xi)} \left\{ -i \sum_{n=2}^{\infty} \frac{\xi^n}{n!} \frac{d^n \psi_0}{d\xi^n} \right. \right. \\ &\quad \left. \left. + \frac{i}{6} \left[\sum_{n=2}^{\infty} \frac{\xi^n}{n!} \frac{d^n \psi_0}{d\xi^n} \right]^3 \right\} \right\rangle. \end{aligned} \quad (6)$$

We substitute expression (6) in (5) and calculate the leading linear terms proportional to a , $\partial a / \partial \tau_0$, $\partial^2 a / \tau_0^2$ as well as the nonlinear term proportional to $|a|^2 a$. After some algebra, we obtain

$$\begin{aligned} \frac{\partial a}{\partial \tau_s} + \frac{1}{2} a &= \frac{\hat{I}}{4v} \left[G_0(p_0) a - i G_1(p_0) \varepsilon \frac{\partial a}{\partial \tau_0} \right. \\ &\quad \left. - \frac{1}{2} G_2(p_0) \varepsilon^2 \frac{\partial^2 a}{\partial \tau_0^2} + \beta(p_0) |a|^2 a \right], \end{aligned} \quad (7)$$

where

$$\begin{aligned} G_0(p_0) &= \frac{1}{2} \frac{d}{dp_0} \left(\frac{\cos p_0 - 1}{p_0^2} \right) + \frac{i}{2} \frac{d}{dp_0} \left(\frac{p_0 - \sin p_0}{p_0^2} \right), \\ G_1(p_0) &= \frac{dG_0}{dp_0}, \quad G_2(p_0) = \frac{d^2 G_0}{dp_0^2}. \end{aligned}$$

Note that the real part G_{0r} is just the standard FEL small-gain function which is positive for $0 < p_0 < 6.28$ with a maximum at $p_0 \approx 2.6$. The coefficient β is complicated and cannot be written in closed form, but we can express it as a power series in p_0 , that is, $\beta(p_0) = \sum_n \beta_n p_0^n$. We have calculated the coefficient β_n using Mathematica up to $n = 25$, and find that $\beta(p_0)$ is well approximated by the relation $\beta(p_0) \approx -2.3 |G_0(p_0)|^2 G_0(p_0)$, for $|p_0| < 6$. Equation (7) can be reduced to the standard form (1) of the GLE by means of the following transformations: $a = A_0 A \exp[i(\kappa z + \Omega t)]$ and $\tau_s = z_0 z, \tau_0 = t_0 t - \tau_s / v_0$, where $z_0 = 2 / [\hat{I}(G_{0r} - G_{1r}^2 / 2G_{2r}) / 2v - 1]$, $1/v_0 = \hat{I} \varepsilon (G_{1i} - G_{1r} G_{2i} / G_{2r}) / 4v$, $\kappa = \hat{I} z_0 (G_{0i} - G_{1r}^2 G_{2i} / 2G_{2r}) / 4v$, $A_0^2 = -4v / z_0 \hat{I} \beta_r$, $t_0^2 = -\varepsilon^2 z_0 \hat{I} G_{2r} / 8v$, $\Omega = -G_{1r} t_0 / \varepsilon G_{2r}$ with $c_1 = G_{2i} / G_{2r}$, $c_2 = \beta_i / \beta_r$.

Single-mode solutions of (1) and their stability properties have been discussed in [7]. The single mode with the largest gain is stable, that is, there is no Benjamin-Feir instability [9] of the GLE if $1 + c_1 c_2 > 0$, which is valid for $|p_0| < 4.632$. However, away from the gain maximum, the system is unstable to the Eckhaus instability [9]. Following the method discussed in [7], we can obtain analytically the following stability condition for $\varepsilon \rightarrow 0$:

$$\left(1 + \frac{G_{2i} \beta_i}{G_{2r} \beta_r} \right) |a_0|^2 > \frac{G_{1r}^2}{G_{2r} \beta_r} \left(1 + \frac{\beta_i^2}{\beta_r^2} \right). \quad (8)$$

Here

$$|a_0|^2 = \frac{1}{\beta_r} \left[\frac{G_m}{\chi} - G_{0r} \right] \quad (9)$$

is the square of amplitude of the complex saturated radiation field, G_m is a constant chosen to be close to the maximum value of G_{0r} , and $\chi \equiv G_m \hat{I} / 4v$. Note that it is always possible to choose $|a_0|^2$ so that the Eckhaus stability condition (8) is violated. As shown in [7], the Eckhaus instability is essentially a phase instability, that is, the phase perturbation grows much faster than the amplitude perturbation in the linear regime.

In Fig. 1, we plot contours of constant χ (dashed lines), calculated from (9) in (a_0, p_0) space. This plot is qualitatively similar to that calculated in [5] using the basic equations (3) and (4), and gives confidence in the predictive capability of the GLE. When $\varepsilon > 0$, the analytical condition (8) is not accurate for small $|a_0|$, and so we determine the stable domain numerically. The solid lines in Fig. 1 define the stability boundaries for $\varepsilon = 0.2$, with the stable region lying between the two lines. The dotted line in Fig. 1 represents the stability boundaries according to the analytical condition (8) which is valid in the limit $\varepsilon \rightarrow 0$. For small but nonzero values of ε (for example, $\varepsilon \approx 3.3 \times 10^{-3}$ for the UCSB FEL), the numerical stability boundaries cannot be distinguished from the $\varepsilon \rightarrow 0$ boundaries when plotted on the scale of Fig. 1.

In [7], we have presented numerical simulations for the GLE showing that it takes a rather long time, compared with the electron pulse length, for the radiation field to relax to a single-mode state. While the amplitude relaxes quickly to a near-constant value, multiple modes persist in the phase. This can be easily explained by the fact that the decay rate of the amplitude perturbation is much larger than that of the phase perturbation. The spectral half-width of the radiation field is found to decay as $\tau_s^{-1/2}$, in agreement with [5].

Danly *et al.* [2] have reported direct observations of the UCSB FEL spectrum with a spectrometer that can resolve 20 modes in a given pulse. About 90 spectra were taken, and 29% of them were found to be a “single-mode” state, defined in [2] as a state in which one mode has power at least twice as large as any other mode. Note that this is a much less stringent definition of a single-mode state than we have adopted so far. We now compare

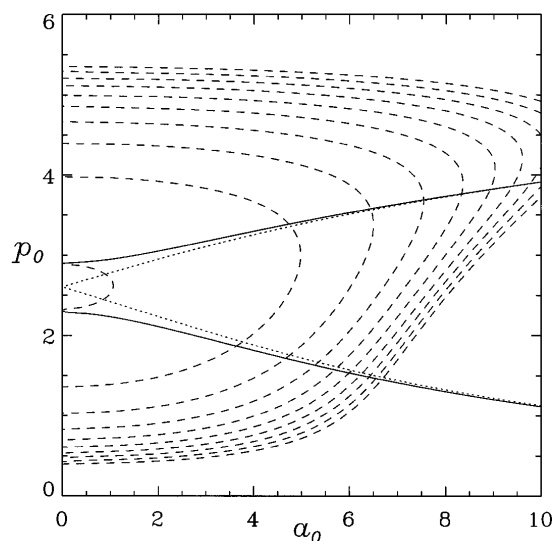


FIG. 1. Contours of constant χ (dashed curves) plotted in (a_0, p_0) space for the parameters of the UCSB FEL, calculated using (9). The phase stability boundary for $\varepsilon = 0.2$ (solid curve) and $\varepsilon \rightarrow 0$ (dotted curve) is calculated using (8). The central region is stable.

these spectral observations with simulations of the GLE using random initial conditions. In all runs, we used parameters characteristic of the UCSB experiment, with $\varepsilon = 3.3 \times 10^{-3}$, $p_0 = 2.606$ which is near maximum gain with $G_m = G_{0r}$ (2.606, and $\chi = 3$). We use periodic boundary conditions on τ_0 (with a period of 2) and a total of 1024 Fourier modes, including 390 modes under the positive gain curve. Initially, random small amplitudes are assigned to all Fourier modes, and the radiation field is calculated as a function of τ_s by solving (7) numerically using a pseudospectral method. Assuming $v_g \approx c$, we obtain the slow time $\tau_s = tv v_g / 2L_c \approx tv / 0.05 \mu\text{s}$. Since v is the fractional power loss per round trip, its maximum value is one. The maximum time t is determined by the pulse length of the electron beam, which is about $50 \mu\text{s}$. Hence, we run the numerical experiments for $\tau_s \leq 1000$. In reality, since v is smaller than unity, τ_s is of the order of a few hundred.

We present the statistical results from 10^4 runs, each with a random initial condition. In Fig. 2, we plot the probability P_{20} (solid line) of finding a “single mode” within the central 20-mode range (defined in [2] and [10]) as a function of τ_s . We see that the probability grows very rapidly for $\tau_s < 50$, but grows much more slowly after that at a level about 10%. This agrees with the estimates given in [10] but is about one-third of the experimental finding [2]. It is possible that the discrepancy between theory and experiment can be accounted for by invoking a frequency-dependent reflection coefficient of the cavity, considered below in greater detail in the context of the Dutch experiment.

In Fig. 2(a), the dotted line represents P_{all} , the probability of a single mode for the entire spectrum. Note that, by definition, we must have $P_{\text{all}} \leq P_{20}$. We see that there exists a substantial difference (about 0.04) between the two curves for τ_s as large as 400. This implies that about one-third of the so-called single-mode cases, inferred by calculating P_{20} , are not, in fact, true single modes even by the less stringent definition adopted in [2] because it

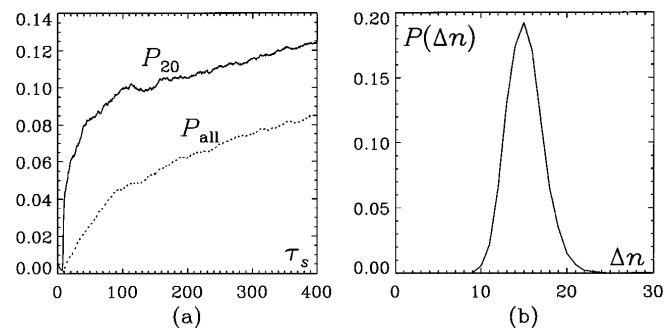


FIG. 2. (a) Solid curve: the probability P_{20} of obtaining a single mode using the less stringent definition of [3] and [10], within the central 20-mode range as a function of τ_s based on 10^4 random runs. Dotted curve: the probability P_{all} of a single mode for the whole spectrum. (b) Probability density $P(\Delta n)$ at $\tau_s = 400$ based on the same set of runs as in (a).

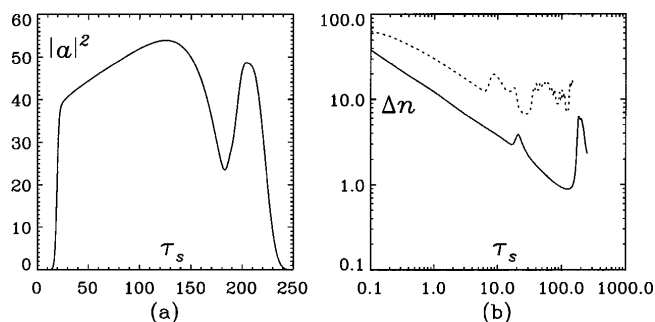


FIG. 3. (a) $|a|^2$ as a function of τ_s from a simulation of the GLE for parameters of the Dutch fusion FEM experiment, including the effects of a frequency-dependent reflection coefficient and time-dependent p_0 . (b) Number of modes in the spectrum Δn (solid curve), defined in text, as functions of τ_s . The dashed curve represents Δn for a run with identical parameters but without the frequency dependence.

is possible to find a mode with a larger amplitude outside the central 20-mode range. In fact, if we determine single-mode states by the more stringent and accurate condition $\Delta n < 1$, where $\Delta n = \langle (n - \langle n \rangle)^2 \rangle^{1/2}$, with $\langle n \rangle = \sum_n n |a_n| / \sum_n |a_n|$, the probability density $P(\Delta n)$, shown in Fig. 2(b) (for $\tau_s = 400$), peaks at about $\Delta n \approx 15$ with a deviation of about ± 5 . The probability for Δn to be near 1, representing a true single-mode state, is negligibly small.

We now turn to a discussion of the recently reported possible single-mode operation in the Dutch fusion FEM [3]. An important feature that we take into account in the interpretation of this experiment is the frequency dependence of the reflection coefficient of the waveguide cavity reflector. This coefficient has a value of about 0.5 at a central frequency of about 200 GHz from where it falls off approximately linearly to about 0.2 in a 10 GHz interval on both sides of the central frequency [11]. We can model this frequency-dependent cavity loss by replacing the second term on the left-hand side of (7) by the term

$$\frac{1}{2} \left[d_0 a - i d_1 \varepsilon \frac{\partial a}{\partial \tau_0} - \frac{1}{2} d_2 \varepsilon^2 \frac{\partial^2 a}{\partial \tau_0^2} \right],$$

where d_0, d_1, d_2 are complex constants chosen such that the minimum normalized cavity loss coefficient over all frequency is equal to $\frac{1}{2}$. Note that the modified equation is still in the Ginzburg-Landau form [1], except that the coefficients are changed. In the experiment, the resonant frequency shifts slowly to lower values because the electron energy drops slowly. We model this effect in (7) by letting p_0 increase linearly with τ_s .

In Fig. 3(a), we show the power $|a|^2$ as a function of τ_s in a GLE simulation with parameters $\varepsilon = 0.02, \chi = 3$.

Note that, for $\nu = 0.75$, $\tau_s = 250$ corresponds to about 10 μs in real time, similar to the time scale of the fusion FEM experiment. The double-peak feature is indeed seen in the experiment [3]. In Fig. 3(b), we plot Δn , defined above, as a function of τ_s . The solid curve represents Δn including the frequency-dependent reflection coefficient, whereas the dashed curve represents Δn without the frequency dependence in the cavity loss term, that is, with $d_0 = 1$ and $d_1 = d_2 = 0$. Figure 3(b) shows clearly that, without the frequency-dependent reflection coefficient, Δn remains a larger value than unity due to the excitation of Eckhaus instabilities as the amplification band shifts. However, with the frequency-dependent reflection coefficient, the single-mode criterion $\Delta n < 1$ is satisfied at about $\tau_s = 100$. Thereafter, the system becomes Eckhaus unstable at about $\tau_s = 150$. Δn increases quickly, increasing the intensity of the total radiation field and causing the second peak seen in Fig. 3(a). Subsequently, the FEL shows a second relaxation phase to a single-mode state, but does not have time to attain $\Delta n < 1$ since the amplification band shifts through the cavity band altogether and the total power dies out quickly.

This research is supported by the Air Force Office of Scientific Research Grant No. F49620-96-1-0068 and the Department of Energy Grant No. DE-FG02-91ER40669.

-
- [1] L.R. Elias, G. Ramian, J. Hu, and A. Amir, *Phys. Rev. Lett.* **57**, 424 (1986); L.R. Elias and I. Kimel, *Nucl. Instrum. Methods Phys. Res., Sect. A* **296**, 144 (1990).
 - [2] B.G. Danly *et al.*, *Phys. Rev. Lett.* **65**, 2251 (1990).
 - [3] W.H. Urbanus *et al.*, *Nucl. Instrum. Methods Phys. Res., Sect. A* (to be published).
 - [4] I. Kimel and L.R. Elias, *Phys. Rev. A* **38**, 2889 (1988); *Nucl. Instrum. Methods Phys. Res., Sect. A* **296**, 528 (1990); **341**, 191 (1994).
 - [5] B. Levush and T.M. Antonsen, Jr., *Nucl. Instrum. Methods Phys. Res., Sect. A* **272**, 375 (1988); **285**, 136 (1989); T.M. Antonsen, Jr. and B. Levush, *Phys. Rev. Lett.* **62**, 1488 (1989); *Phys. Fluids B* **1**, 1097 (1989).
 - [6] S.Y. Cai and A. Bhattacharjee, *Phys. Rev. A* **43**, 6934 (1991).
 - [7] C.S. Ng and A. Bhattacharjee, *Phys. Rev. E* **58**, 3826 (1998).
 - [8] Ya.L. Bogomolov *et al.*, *Opt. Commun.* **36**, 109 (1981).
 - [9] J.T. Stuart and R.C. DiPrima, *Proc. R. Soc. London A* **362**, 27 (1978); B.I. Shraiman *et al.*, *Physica (Amsterdam)* **57D**, 241 (1992); T. Leweke and M. Provansal, *J. Fluid Mech.* **288**, 265 (1995).
 - [10] T.M. Antonsen, Jr., and B. Levush, *Phys. Fluids B* **2**, 2791 (1990).
 - [11] V.L. Bratman *et al.*, *Nucl. Instrum. Methods Phys. Res., Sect. A* **407**, 40 (1998).